ChemPubSoc Europe

DOI: 10.1002/chem.201503981

CHEMISTRY
A European Journal
Full Paper

Drug Discovery | *Hot Paper*

An Aromatic Hydroxyamide Attenuates Multiresistant *Staphylococcus aureus* Toxin Expression

Jan Vomacka,[b] Vadim S. Korotkov,[b] Bianca Bauer,[b] Franziska Weinandy,[b] Martin H. Kunzmann,[a] Joanna Krysiak,[a] Oliver Baron,[c] Thomas Böttcher,[d] Katrin Lorenz-Baath,[b] and Stephan A. Sieber*[a]

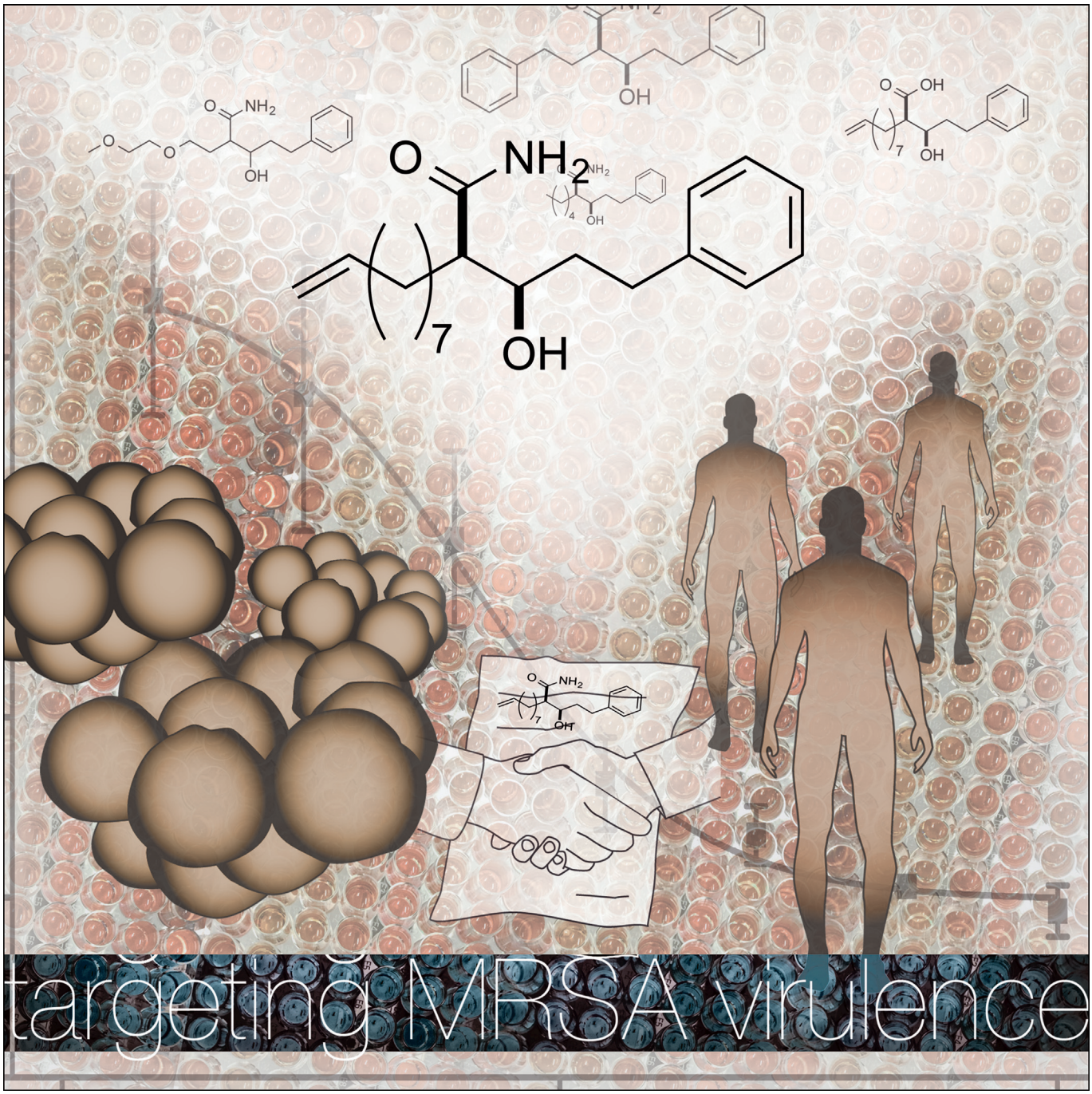

Abstract: Methicillin-resistant *Staphylococcus aureus* (MRSA) causes severe infections with only few effective antibiotic therapies currently available. To approach this challenge, chemical entities with a novel and resistance-free mode of action are desperately needed. Here, we introduce a new hydroxyamide compound that effectively reduces the expression of devastating toxins in various *S. aureus* and MRSA strains. The molecular mechanism was investigated by transcriptome analysis as well as by affinity-based protein profiling. Down-regulation of several pathogenesis associated genes suggested the inhibition of a central virulence-related pathway. Mass spectrometry-based chemical proteomics revealed putative molecular targets. Systemic treatment with the hydroxyamide showed significant reduction of abscess sizes in a MRSA mouse skin infection model. The absence of resistance development in vitro further underlines the finding that targeting virulence could lead to prolonged therapeutic options in comparison to antibiotics that directly address bacterial survival.

Introduction

The spread of methicillin-resistant *Staphylococcus aureus* (MRSA) poses a major threat to public health and represents one of the greatest challenges for clinicians today.[1] In addition to the ability of MRSA to cause life-threatening diseases such as endocarditis, pneumonia, or sepsis as well as severe skin and soft tissue infections, its high mutation frequency by which it rapidly accumulates multiple antibiotic resistances, is of major concern.[2]

Alternative treatment strategies targeting bacterial pathogenicity are emerging, that is, inhibiting virulence instead of bacterial viability.[3,4] Bacterial virulence is determined by a diverse set of molecules, including toxins and adhesins, which are needed to establish and propagate infection.[5] Inhibition of central virulence pathways disarms bacteria without directly affecting their viability, thus leading to less selective pressure and decreased resistance development.[6–10] Several mouse studies have already confirmed the success of this concept by showing that anti-virulence compounds improve the outcome of *S. aureus* induced sepsis, pneumonia or skin infections.[11–15] These approaches addressed very different targets—from interference with cholesterol biosynthesis[11–13] to the inhibition of toxins[14,15] or cell adhesion.[16] Moreover, the efficacy of therapeutic antibodies that block diverse virulence determinants of *S. aureus* has been reported from animal studies.[17,18] However, immunotherapeutics against a single virulence factor were only moderately effective in phase 1 or 2 clinical trials; therefore, current approaches are starting to combine multiple antibody formulations directed against a series of key staphylococcal toxins.[18] Consequently, we focused our study on the discovery of anti-virulence small molecules that inhibit not only one but multiple staphylococcal virulence factors.

S. aureus virulence is controlled by complex pathways such as the accessory gene regulator (agr) two-component system.[19] Small autoinducing peptides (AIPs), encoded by agrD, are secreted and sensed by a growing population.[19] Once a critical density is reached, AIPs bind to histidine kinase AgrC on the cell surface and induces phosphorylation of an intracellular response regulator (AgrA) to activate transcription of RNAIII, which is an effector of a broad range of diverse virulence factors.[20] Synthetic derivatives of AIPs have been shown to effectively repress this sensing mechanism.[21–23] In addition, staphylococcal accessory regulator (SarA) and homologous proteins such as SarX independently control the transcription of toxins through direct binding to promoter regions.[24,25]

Herein we report the identification of a new chemical virulence inhibitor (*R**,*R**)-**3** (Figure 1a), bearing an aromatic hydroxyamide functional group that blocks a variety of different staphylococcal virulence factors. Systemic treatment with the inhibitor in mice led to a significant reduction of MRSA induced skin abscesses. Together with the lack of in vitro resistance development of (*R**,*R**)-**3** treated bacteria, the new compound represents a promising starting point for further medicinal development.

Results and Discussion

Hydroxyamide (*R**,*R**)-3 broadly inhibits virulence factors of *S. aureus* in multiresistant clinical isolates

In previous studies we identified β-lactones as specific inhibitors of bacterial caseinolytic protease P (ClpP), which is a virulence associated protein, that attenuates pathogenicity in bacterial cultures as well as in a murine infection model.[15,26]

[a] *Dr. M. H. Kunzmann, Dr. J. Krysiak, Prof. S. A. Sieber*
Department of Chemistry, Chair of Organic Chemistry II
Center for Integrated Protein Science (CIPSM)
Institute of Advanced Studies (IAS), Technische Universität München (TUM)
Lichtenbergstrasse 4, 85747 Garching (Germany)
E-mail: stephan.sieber@tum.de

[b] *J. Vomacka, Dr. V. S. Korotkov, Dr. B. Bauer, Dr. F. Weinandy, Dr. K. Lorenz-Baath*
Department of Chemistry, AVIRU, GO-Bio-project of the Federal Ministry of Education and Research, FKZ: 031A131
Technische Universität München (TUM)
Lichtenbergstrasse 4, 85747 Garching (Germany)

[c] *Dr. O. Baron*
Department of Chemistry, Center for Integrated Protein Science (CIPSM)
Ludwig-Maximilians-Universität München (LMU)
Butenandtstrasse 5–13, 81377 Munich (Germany)

[d] *Dr. T. Böttcher*
Department of Chemistry, Universität Konstanz
Universitätsstrasse 10, 78457 Konstanz (Germany)

Supporting information, including detailed experimental descriptions for all experiments, and ORCID(s) from the author(s) for this article are available on the WWW under http://dx.doi.org/10.1002/chem.201503981.

Further progress was mainly limited by the low plasma stability of the β-lactones.[15] In the search for antivirulence compounds with improved pharmacological properties, we opened the lactone ring of **1** through hydrolysis or aminolysis to obtain open-chain β-hydroxyacid **2** and β-hydroxyamide **3**, respectively, both as (*R**,*R**)-diastereomers (Figure 1a). Initially, the biological activity of the newly synthesized substances was investigated. To rule out an antibiotic mode of action and focus on substances with antivirulence activity, we performed a minimum inhibitory concentration (MIC) test with *S. aureus* (NCTC 8325). Only compound **2** exhibited a MIC of 400 μM (127 μg mL^{-1}), and was thus excluded from further investigations (Figure 1a). Given that no inhibition of bacterial growth was obtained after treatment with (*R**,*R**)-**3** up to concentrations of 1 mM (317 μg mL^{-1}), we focused on this compound for further studies.

Hemolysin alpha (hla), a pore-forming cytotoxin that causes lysis of immune cells and erythrocytes, is one of the major staphylococcal virulence factors. Remarkably, (*R**,*R**)-**3** inhibited hemolytic activity of two major *S. aureus* strains (NCTC 8325 and MRSA USA 300) with EC_{50} values of 13 μM (4.1 μg mL^{-1}; Figure 1b) and 18 μM (5.7 μg mL^{-1}; see the Supporting Information, Figure S1a), respectively. Western blot analysis revealed that reduced hemolysis was based on decreased production of hla (Figure 1b and Figure S1a). Importantly, a broad spectrum of 16 independent clinical isolates from different disease origins containing different resistance types (methicillin-sensitive *S. aureus* (MSSA) and methicillin-resistant *S. aureus* (MRSA)) were largely sensitive to treatment with (*R**,*R**)-**3**, showing reduced hemolysis of erythrocytes (Figure 1c). Whereas some isolates did not show effective hemolysis at all (BK97296, VA402525, VA417350, VA12350), only two haemolytic strains did not respond to the treatment with (*R**,*R**)-**3**. Importantly, the production of sepsis causing toxic shock syndrome toxin (TSST-1) was also decreased with an EC_{50} of 7 μM (2.22 μg mL^{-1}) in TSST-1 producing strain Mu 50 (Figure 1d). In addition, (*R**,*R**)-**3** attenuated the production of other staphylococcal virulence factors, including diarrhea causing enterotoxins (SAE A-E; see the Supporting Information, Figure S1b) in a concentration-dependent manner. Furthermore, the (*R**,*R**)-**3** mediated inhibition of toxin secretion led to a protection of eukaryotic, alveolar cells from cell death in an in vitro model of *S. aureus* toxin-induced cell injury during lung infection (see the Supporting Information, Figure S1c).

To investigate structure-activity relationships we tested various hydroxyamide derivatives. Several analogues featuring aromatic and aliphatic substituents as putative protein-binding ligands were synthesized according to two different routes (Scheme 1). In brief, β-lactone ring-opening reactions with ammonia in isopropanol stereoselectively led to the desired compounds (Route I). *trans*-β-Lactones were obtained by $ZnCl_2$-catalyzed tandem Mukaiyama aldol-lactonization (TMAL)[27,28] from aldehydes and ketene acetals. Alternatively, hydroxyamides were synthesized by utilizing aldol condensation (Route II). Given that the reaction is not stereoselective, a mixture of both diastereomers was formed; these were successfully separated by column chromatography and further converted into

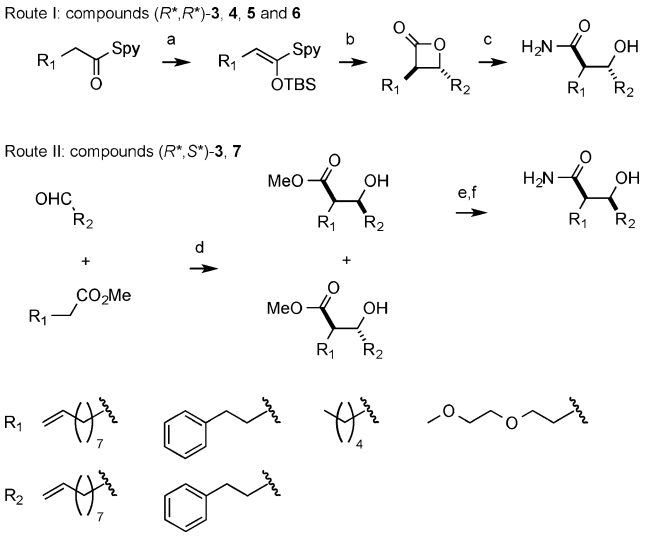

Scheme 1. Two routes for the synthesis of hydroxyamide derivatives. Reagents and conditions: a) TBSCl, LHMDS, Et_3N, THF, DMF, −78 to 0 °C, 2 h; b) $ZnCl_2$, R_2CHO, CH_2Cl_2, RT, 4 d; c) NH_3 in *i*PrOH, RT, 18 h; d) LHMDS, THF, −78 °C, (no separation of diastereomers for compound **7**; e) NaOH, H_2O, MeOH, RT, 18 h; f) NH_4HCO_3, Boc_2O, py, CH_3CN, RT, 18 h. TBS = tri-*n*-butylsilyl; LHMDS = lithium hexamethyldisilazide.

the desired compounds. The effect of the derivatives on hla inhibition was examined by hemolysis assay (Figure 1e). Interestingly, diastereomer (*R**,*S**)-**3** was almost inactive. In addition, the orientation of both side chains was crucial for anti-hemolytic activity, because substance **4**, with exchanged substituents, showed a reduced effect in the hemolysis assay. All attempts to replace the nonenyl chain, for example, by the introduction of pentyl (**5**), phenylethyl (**6**), or 1-ethoxy-2-methoxyethane (**7**), resulted in molecules with impaired activity compared with (*R**,*R**)-**3** (Figure 1e).

Unlike the parent β-lactones,[15,26] (*R**,*R**)-**3** did not inhibit ClpP activity in vitro (see the Supporting Information, Figure S2), suggesting a different antivirulence mode of action.

Transcriptome analysis revealed a strong impact of (*R**,*R**)-3 treatment on virulence factor regulation

To elucidate the inhibitory molecular mechanisms of (*R**,*R**)-**3**, next generation sequencing was applied to analyze transcriptional changes of NCTC 8325 cells after treatment with (*R**,*R**)-**3**. Cells treated with dimethyl sulfoxide (DMSO) were used as control. Significant (>1 or <-1 $\log_2$ fold change, $p<0.05$) regulation of 197 genes (6.9% of all genes) was observed, with 149 genes being down-regulated and 48 being up-regulated (Figure 2a). A DAVID database[29,30] gene cluster analysis based on gene annotation terms revealed that a substantial number of down-regulated genes clustered within the pyruvate metabolism, metal ion binding processes, and virulence associated mechanisms (see the Supporting Information, Figure S3). Remarkably, several enzymes connecting glycolysis with the citrate acid cycle via pyruvate were significantly down-regulated, suggesting a strong effect on central carbon metabolism. Consistent with the antihemolytic effect, hla transcript levels were

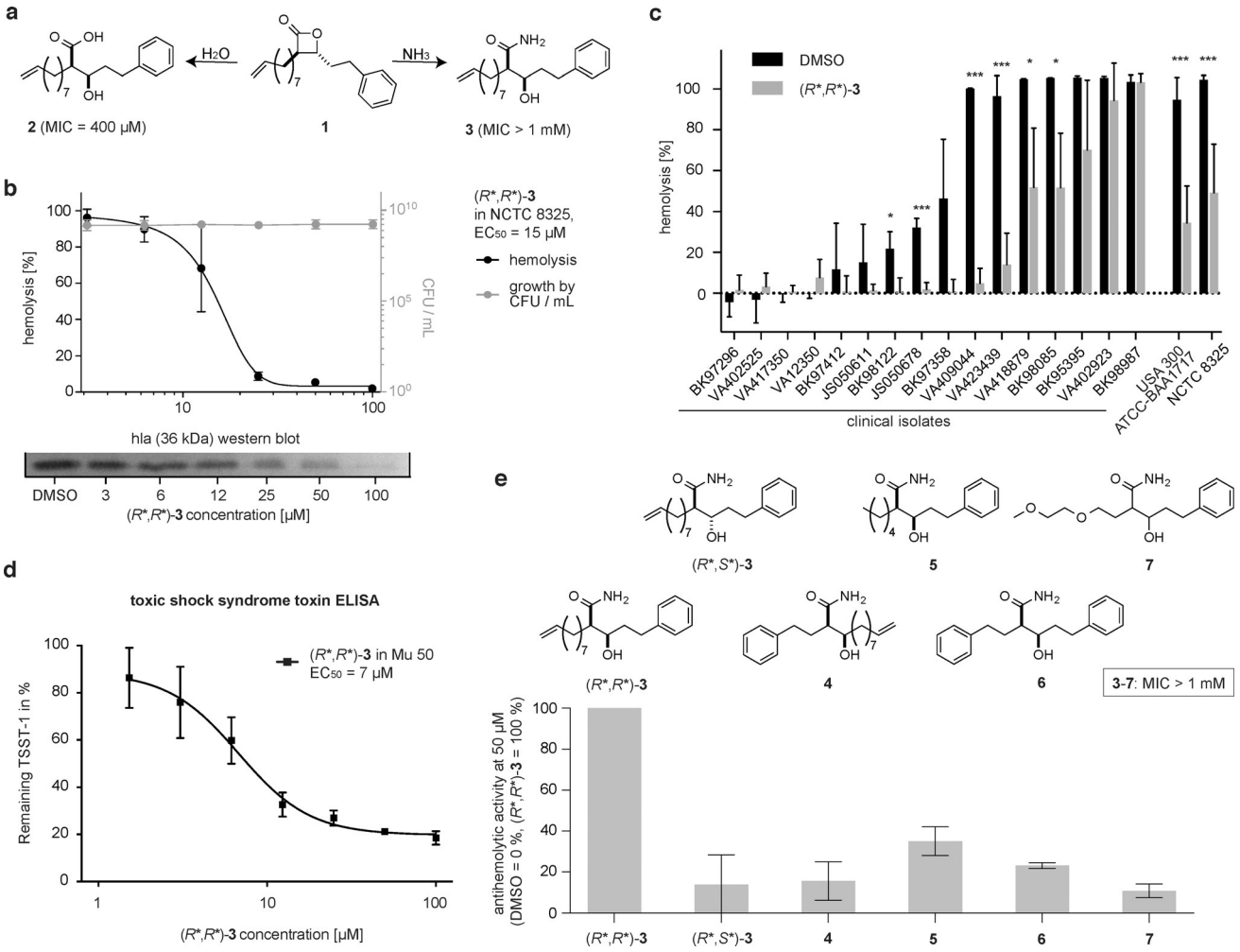

Figure 1. (*R**,*R**)-**3** strongly inhibits hemolysis in *S. aureus*. a) Ring opening of anti-virulence compound **1** through hydrolysis or aminolysis yields an open chain β-hydroxyacid **2** and β-hydroxyamide **3**, respectively, both as (*R**,*R**)-diastereomers. Antibiotic effects were determined by measuring minimum inhibitory concentrations (MIC) up to 1 mM for three biological replicates. b) Hemolysis inhibition with (*R**,*R**)-**3** in *S. aureus* NCTC 8325. The mean value of three technical replicates is shown. These findings were further confirmed by western blot analysis of hla (lower panel). Growth is indicated by colony-forming units (CFU)/mL culture. c) Inhibition of hemolysis by 100 μM (*R**,*R**)-**3** in clinical isolates originating from blood cultures (BK95395#, BK98122, BK98085, BK97358, BK97472, BK97296#, BK98987), abscesses (VA423439, VA409044#, VA402525#, VA402923#, VA412350#) and pneumonia (VA418879#, IS050611#, IS050678#, VA417350#). MRSA strains are marked by (#). The mean value of three biological replicates ± SD is shown. Significant difference of compound treated compared with DMSO control treated samples (one-sample Student's t-test, * $p < 0.05$, *** $p < 0.001$). d) Toxic shock syndrome toxin 1 (TSST-1) reduction by (*R**,*R**)-**3** in *S. aureus* Mu 50 was detected by ELISA in three biological replicates. e) Structures of anti-virulence compounds and their derivatives used for structure activity relationship studies (**1**–**7**) and target identification (**8**). Antibiotic effects were determined by measuring minimum inhibitory concentrations (MIC) up to 1 mM for three biological replicates. Antihemolytic activity of hydroxyamide derivatives (50 μM) **3**–**7**: Measurements were normalized according to DMSO control (0% activity) and (*R**,*R**)-**3** (100% activity). The mean value of at least three biological replicates ± SD is shown.

3.29 fold reduced (1.72 $\log_2$ fold). Several major virulence-associated transcriptional activators such as SarA and SarR[31] were among the strongest down-regulated genes (Figure 2b and Figure S3in the Supporting Information). In contrast, SarX,[25] a negative regulator of agr promoted virulence, was found to be the only virulence-associated up-regulated gene. Thus, transcriptional analysis supports the global antivirulence properties of (*R**,*R**)-**3**.

Chemical proteomics reveal target proteins

To identify protein target(s) of (*R**,*R**)-**3**, we synthetically equipped the active and inactive core structures (*R**,*R**)-**3** and (*R**,*S**)-**3** with an alkyne handle at the terminal end of the alkyl chain, and replaced the phenyl ring with a benzophenone photocrosslinker (Scheme 2). Synthesis started with the Heck reaction of the protected 4-bromobenzophenone with acrylic acid. The product obtained was hydrogenated and converted into the corresponding aldehyde. Its aldol reaction with TMS-protected methyl undec-10-ynoate yielded a mixture of two diastereomeric 3-hydroxyesters. Diastereomers of the 3-hydroxyacid obtained after deprotection steps were separated by column chromatography and converted into the desired photo-probes (*R**,*R**)-**8** and (*R**,*S**)-**8**.

The functionalized affinity-based protein profiling (AfBPP) probe[32] (*R**,*R**)-**8** retained anti-hemolytic properties, albeit

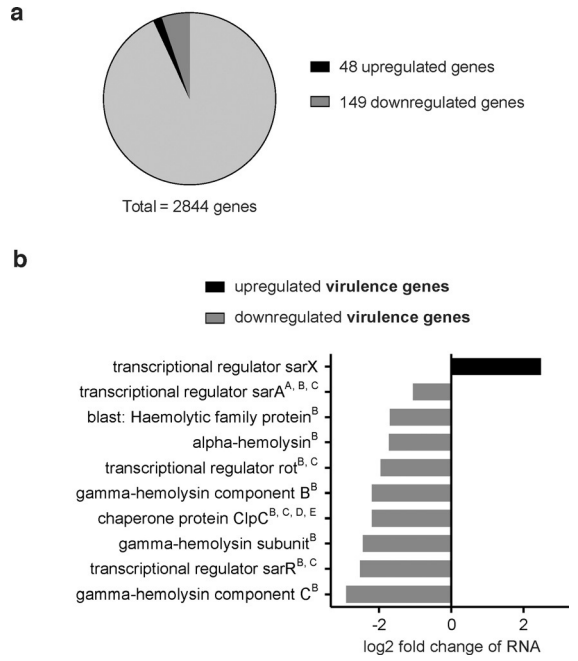

Figure 2. Next generation sequencing of NCTC 8325 cells treated with 100 μM (31.7 μg mL^{-1}) (*R**,*R**)-**3** compared with DMSO control. a) Fraction of up- and down-regulated genes (>1 or <-1 $\log_2$ fold change, *p*-value <0.05). b) Up- and down-regulated virulence associated genes. Virulence genes were identified by searching the DAVID[29,30] functional annotation table for the terms: virulence, pathogenesis, cell killing and cytolysis. For regulated DAVID database gene clusters, see the Supporting Information (Figure S3). A–E: gene is part of the following DAVID gene clusters (enrichment score): A: metal ion binding (2.27); B: virulence (2.26); C: virulence regulation (0.80). D: DNA repair, stress response (0.43); E: nucleotide binding (0.41). See also the supporting transcriptome analysis.xlsx file.

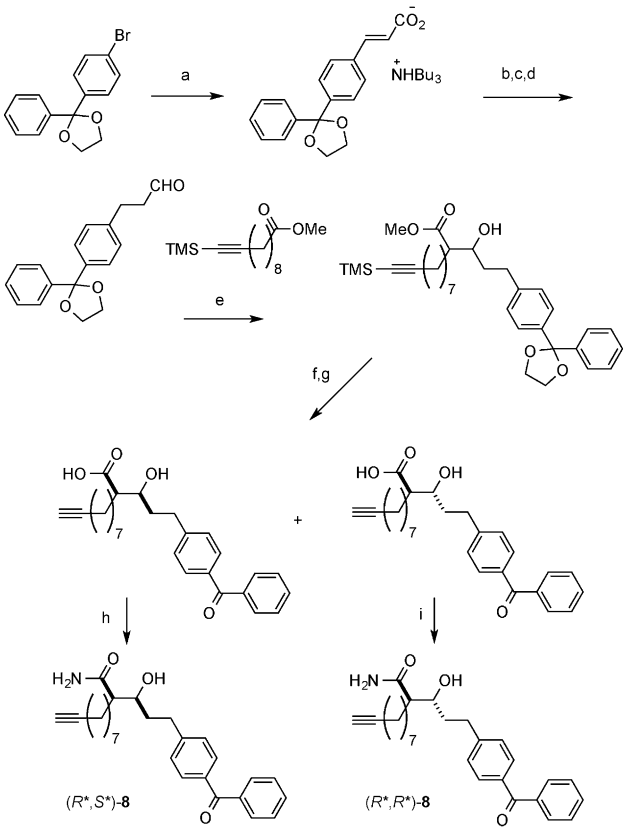

Scheme 2. Synthesis of the affinity-based protein profiling (AfBPP) probes. Reagents and conditions: a) acrylic acid, $Pd(OAc)_2$, Bu_3N, $P(2\text{-}MeC_6H_4)_3$, *o*-xylene, H_2O, 150 °C, 5 h, 74%; b) H_2/Pd/C, MeOH, RT, 16 h, 97%; c) $LiAlH_4$, THF, 80 °C, 2 h, 50%; d) PCC, CH_2Cl_2, RT, 4 h, 80%; e) LHMDS, THF, −78 °C to RT, 4 h, 28%; f) trifluoroacetic acid, RT, 20 h; g) NaOH, THF, H_2O, MeOH, separation of diastereomers; h) NH_4HCO_3, Boc_2O, py, CH_3CN, RT, 22%; i) NH_4HCO_3, Boc_2O, py, CH_3CN, RT, 22%.

with reduced potency compared with the parent structure (Figure 3a). As expected, the (*R**,*S**)-**8** diastereomer was almost inactive. Both probes were incubated with live *S. aureus* (NCTC 8325 and USA 300 Lac) cells and irradiated with UV light to establish a covalent link between the target protein and the photolinker. Cells were lysed and the probe-labeled proteome was modified with fluorescent biotin tags through the use of click chemistry.[33–35] Avidin bead enrichment, SDS-PAGE analysis and fluorescent scanning revealed two intense bands at approximately 90 and 35 kDa (Figure 3b) that were analyzed by LC-MS/MS following tryptic digest. The upper band was identified as 3-hydroxyacyl-CoA dehydrogenase (see the Supporting Information, Figure S4) and the lower band as MntC, which is a binding domain for a manganese membrane transporter (MntABC; see the Supporting Information, Figure S5).

Importantly, labeling with the inactive probe (*R**,*S**)-**8** revealed comparable intensity of the upper band but reduced intensity of the lower band (see the Supporting Information, Figure S6). Labeling in *S. aureus* NCTC 8325 was dose-dependent and the lower band could be detected down to a concentration of 3.5 μM (1.5 μg mL^{-1}) of (*R**,*R**)-**8** (see the Supporting Information, Figure S7).

To comprehensively identify and confirm putative target proteins through quantitative proteomics, we utilized a gel-free approach with dimethyl labeling to introduce light-, medium-, and heavy-isotope tags to peptides after enrichment and digest.[36] Differentially labeled peptides derived from cells treated with the active probe (*R**,*R**)-**8**, the inactive probe (*R**,*S**)-**8** or DMSO, respectively, were mixed and analyzed by MS (see the Supporting Information, Figure S8). Results were ranked according to highest enrichment ratios derived from the active probe in comparison to the DMSO control (Figure 3c) and to the inactive probe (Figure 3d). Only proteins with enrichment higher than one-fold standard deviation (SD) and a *p* value <0.01 were considered. The four hits throughout all experiments were MntC, an uncharacterized esterase, a proline dehydrogenase, and the FtsH metalloprotease (Figure 3e, Supporting Information ABPP_analysis.xlsx file). The 90 kDa 3-hydroxyacyl-CoA dehydrogenase was not enriched by using this method, suggesting that it is an unspecific target of gel-based labeling.

Hit validation was performed by using selective transposon mutants (TN mut.) of *S. aureus* NCTC 8325 that were obtained by phage transduction from USA 300 Lac TN mutant strains from the Nebraska transposon mutant library (NTML, University of Nebraska Medical Center). Fluorescent gel analysis following labeling with (*R**,*R**)-**8** in the MntC-deficient strain revealed

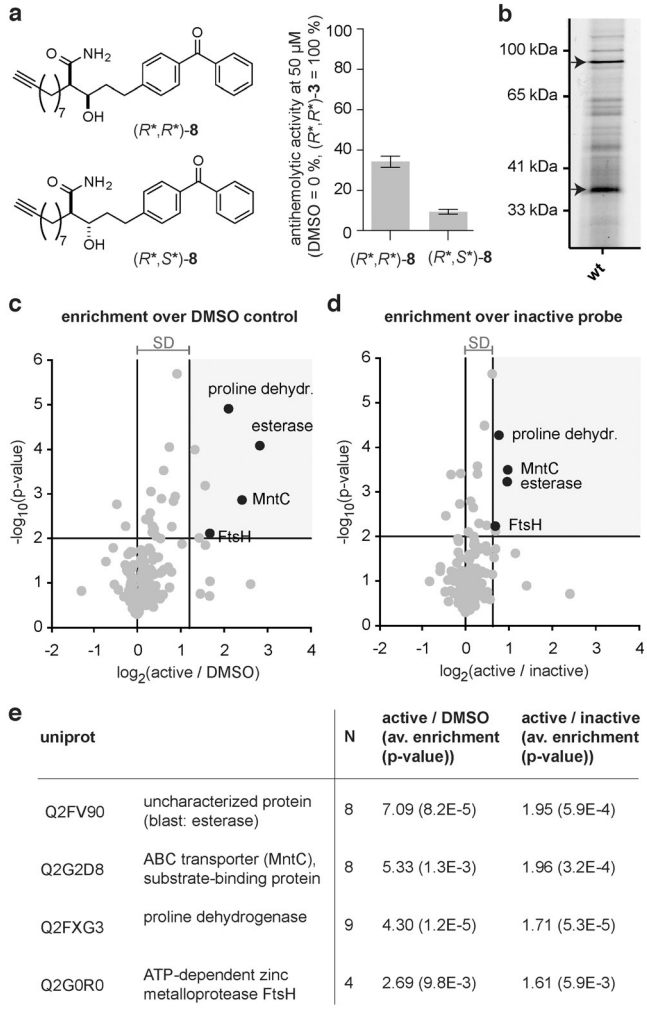

e

uniprot		N	active / DMSO (av. enrichment (p-value))	active / inactive (av. enrichment (p-value))
Q2FV90	uncharacterized protein (blast: esterase)	8	7.09 (8.2E-5)	1.95 (5.9E-4)
Q2G2D8	ABC transporter (MntC), substrate-binding protein	8	5.33 (1.3E-3)	1.96 (3.2E-4)
Q2FXG3	proline dehydrogenase	9	4.30 (1.2E-5)	1.71 (5.3E-5)
Q2G0R0	ATP-dependent zinc metalloprotease FtsH	4	2.69 (9.8E-3)	1.61 (5.9E-3)

Figure 3. MS based target identification. a) Structure and antihemolytic activity of 50 µM photo-probes (*R**,*R**)-**8** and (*R**,*S**)-**8**. Measurements were normalized according to DMSO control (0% activity) and (*R**,*R**)-**3** (100% activity). The mean value of at least three biological replicates ±SD is shown. b) Labeling of NCTC 8325 wt with 50 µM (21.0 µg mL^{-1}) photo-probe (*R**,*R**)-**8**. c), d) Volcano plots showing *p* value ($-\log_{10}$ transformed) and enrichment factor ($\log_2$ transformed) for 35 µM (*R**,*R**)-**8** vs. DMSO control (c) and for (*R**,*R**)-**8** (35 µM) vs. the inactive diastereomer photo-probe (*R**,*S**)-**8** control (35 µM) (d). SD represents the enrichment factor standard deviation over all proteins. Black dots represent proteins that were enriched over both controls. 10 independent biological experiments (five replicates NCTC 8325 and five replicates USA 300 Lac) were performed. Both strains were analyzed together. Separate analysis of each strain can be found in a separate excel file (ABPP_analysis.xlsx). To be considered a hit, the mean of both enrichment factors (active diastereomer (*R**,*R**)-**8** over DMSO and active diastereomer (*R**,*R**)-**8** over inactive diastereomer (*R**,*S**)-**8**) had to be greater than the respective average enrichment factor of all proteins by at least one standard deviation (SD). In addition, the enrichment had to be significant according to a one-sample Student's t-test for enrichment greater than 1 (one-tailed, $p < 0.01$). e) Hits enriched over DMSO and inactive diastereomer photo-probe (*R**,*S**)-**8** control: Uniprot[37] accession numbers and protein names from fasta entries are shown. Uncharacterized proteins were identified by using blast (uniprot). Number of experiments (out of 10 replicates) in which the protein was identified (*N*), average (av.) enrichment factors and corresponding *p* values are shown for both controls.

a similar labeling pattern to that of wild type (wt), except for the loss of the strong fluorescent band at 35 kDa, confirming the previous gel-based assignment of this band as MntC (Figure 4a). To examine the impact of all putative hits revealed by gel-free MS analysis (Figure 3c–e), TN mutations of MntC, the uncharacterized esterase, the proline dehydrogenase, and FtsH were tested for their ability to reduce hemolysis in *S. aureus* USA 300 Lac and NCTC 8325 (Figure 4b). Whereas FtsH and the esterase showed no or only a slight reduction in hemolysis production, respectively, a significant effect was observed for proline dehydrogenase and MntC in the NCTC 8325 strain. It is thus possible that multiple targets are involved in the observed phenotype.

Hydroxyamide (*R**,*R**)-3 does not induce resistance in vitro

Targeting nonessential virulence pathways is believed to decrease selective pressure and limit the development of resistances.[10] To test this concept, the antivirulence compound (*R**,*R**)-**3** and a control antibiotic ofloxacin were compared in a resistance development assay (Figure 5). Bacterial *S. aureus* cultures (NCTC 8325) were treated with either 16 µM (5.2 µg mL^{-1}) (*R**,*R**)-**3** (EC_{50} concentration in the hemolysis assay) or 3.5 µM (1.5 µg mL^{-1}) ofloxacin (no growth inhibition at this concentration based on OD_{600}) over 12 passages. Importantly, whereas treatment with ofloxacin resulted in an increased EC_{50} already after four passages, no change in hemolysis EC_{50} could be observed with the antivirulence compound (*R**,*R**)-**3** (Figure 5). In an independent long-term experiment with (*R**,*R**)-**3**, no resistance development could be observed even after 45 passages (see the Supporting Information, Figure S9).

In vivo efficacy in methicillin-resistant *S. aureus* (MRSA) skin infections

In contrast to β-lactones, which undergo rapid hydrolysis,[15] the related β-hydroxyamide (*R**,*R**)-**3** displayed significantly improved stability in both mouse and human plasma, indicating that it may be suitable for pharmacological application (Figure 6a). We thus evaluated the phase-1 metabolism of (*R**,*R**)-**3** in mouse and human microsomes and observed by LC-MS analysis a dihydroxylation product as the major metabolite. This assignment was confirmed by chemical synthesis of the expected metabolite **9**, which exhibited an identical fragmentation pattern (see the Supporting Information, Figure S10). In vivo pharmacokinetics were performed by using a single dose of 0.42 mg (*R**,*R**)-**3** by intravenous (i.v.) administration in Balb/cOlaHsd mice. Rapid elimination with a half-life of $t_{1/2} = 7.7$ min was observed. Further studies, however, showed that intraperitoneal (i.p.) administration of 3.17 mg of (*R**,*R**)-**3** prolonged the elimination half-life to 4.3 h (Figure 6b). By using a repetitive dosing regimen (three times during 18 h), animals were tightly monitored for clinical symptoms during an explorative toxicity assessment and finally this delivery route was utilized to determine the efficacy of (*R**,*R**)-**3** in an in vivo *S. aureus* mouse abscess model by systemic (i.p.) compound administration. We induced dorsal skin abscesses by subcutaneous infection with MRSA strain USA 300 BAA 1717 in Crl:SKH1-Hr^{hr} hairless mice. To ensure optimal compound availability, we admin-

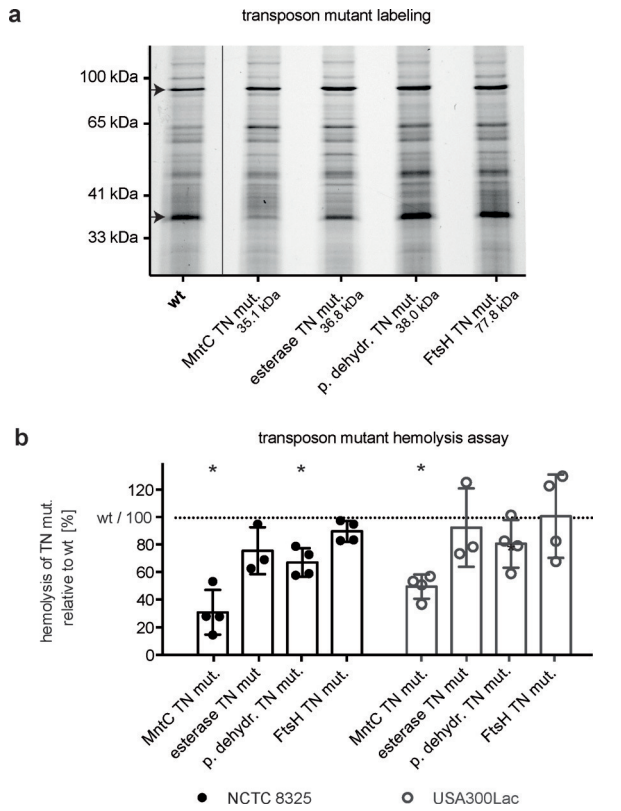

Figure 4. Validation of (*R**,*R**)-**3** targets. a) Labeling of NCTC 8325 wt and transposon mutants (TN mut.) with 50 μM (21.0 μg mL^{-1}) photo-probe (*R**,*R**)-**8**. b) Hemolysis assay of wild type (wt) and transposon mutants (TN mut.) in NCTC 8325 and USA 300 Lac background. * $p < 0.05$ (one sample t test); four biological replicates (three biological replicates for esterase TN mut.).

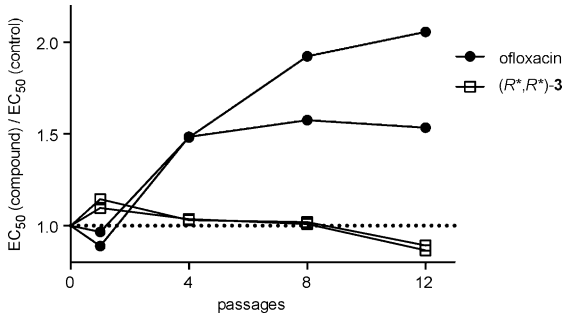

Figure 5. Resistance development assay with antihemolytic compound (*R**,*R**)-**3** (16 μM (5.2 μg mL^{-1})) and ofloxacin (3.5 μM (1.5 μg mL^{-1})). Relative EC_{50} values in hemolysis inhibition of (*R**,*R**)-**3** and growth inhibition of ofloxacin are plotted against the number of passages. Relative EC_{50}: EC_{50} of long-term compound treated bacteria/EC_{50} of long-term vehicle-treated bacteria (DMSO control for (*R**,*R**)-**3** or 0.1 N NaOH control for ofloxacin). The curves for two biological replicates are shown. An independent long-term experiment with compound (*R**,*R**)-**3** with no resistance development over 45 passages is shown in the Supporting Information (Figure S9).

istered the first dose of 3.17 mg (159 mg per kg body weight) (*R**,*R**)-**3** one hour prior to infection and repeated the same dosing six and 18 h after infection (Figure 6c). Abscess lesions were fully developed after one to two days in untreated mice. The necrotic areas were measured over the entire experimental duration for 13 days. The abscess size was significantly decreased to about 60% compared with abscesses obtained in vehicle treated control animals (Figure 6c).

Conclusions

The dramatic increase in bacterial resistance to commonly used antibiotics has been paralleled by a decrease in antibiotic drug development, leading to a poor prognosis for future treatment of infectious diseases. As current antibiotics address only a limited spectrum of essential targets such as cell wall biosynthesis, DNA replication and translation, viability-independent pathways that significantly limit bacterial pathogenesis represent attractive alternatives. Here, we present hydroxyamide (*R**,*R**)-**3** as a potent inhibitor of *S. aureus* virulence. The global reduction of toxin levels such as hla, enterotoxin SAE A-D, and TSST-1, suggests that (*R**,*R**)-**3** hits major target(s) that are responsible for virulence regulation. This observation was further validated by transcriptome analysis of hydroxyamide-treated *S. aureus* cells. Parallel down-regulation of common virulence associated transcriptional activators and up-regulation of the virulence repressor protein SarX was observed. Target identification revealed four protein hits. Among these, proline dehydrogenase and MntC revealed the most significant down-regulation of hemolysis in the NCTC 8325 strain. In fact, MntC is an essential component of the MntABC Mn^{2+} transport system, which consists of an ATP-binding protein (MntA), an integral membrane transporter (MntB), and the metal-binding lipoprotein (MntC).[38,39] A recent study demonstrated severe inhibition of murine systemic infection with a deletion of solely MntC in *S. aureus* USA 300.[40] However, *S. aureus* also encodes MntH, a second manganese uptake system related to the Nramp metal transport family. The individual contribution of both transporters to pathogenesis remains elusive.[41,42]

Future studies will thus investigate a putative synergistic role of other identified targets for the broad antivirulence mechanism. Given the inhibition of devastating toxin expression in various *S. aureus* isolates, the corresponding beneficial effect in a systemic mouse abscess model with an MRSA (USA 300) strain and the lack of resistance development in vitro, aromatic hydroxyamides represent promising starting points for antivirulence drug development.

Experimental Section

Phenotype assays: Bioactivity assays (inhibition of hemolysis, enterotoxins, and TSST) were performed with supernatants from *S. aureus* cultures grown for 20 h at 37 °C. Shortly thereafter, to monitor hemolysis, heparinized sheep blood was added and lysis of erythrocytes was monitored. Enterotoxin and toxic shock syndrome toxin levels in supernatants were determined by ELISA (Ridascreen from R-Biopharm and antibodies from Toxin Technology). Detection of α-hemolysin was performed by Western Blot analysis using ab50536 (Abcam) as the primary antibody. For the long-term resistance assay, cultures were passaged daily with an inoculum of each 3.4×10^4 colony-forming units. Animal experiments were performed with Balb/cOlaHsd (Harlan) and Crl:SKH1-Hr^{hr} (Charles River) mice.

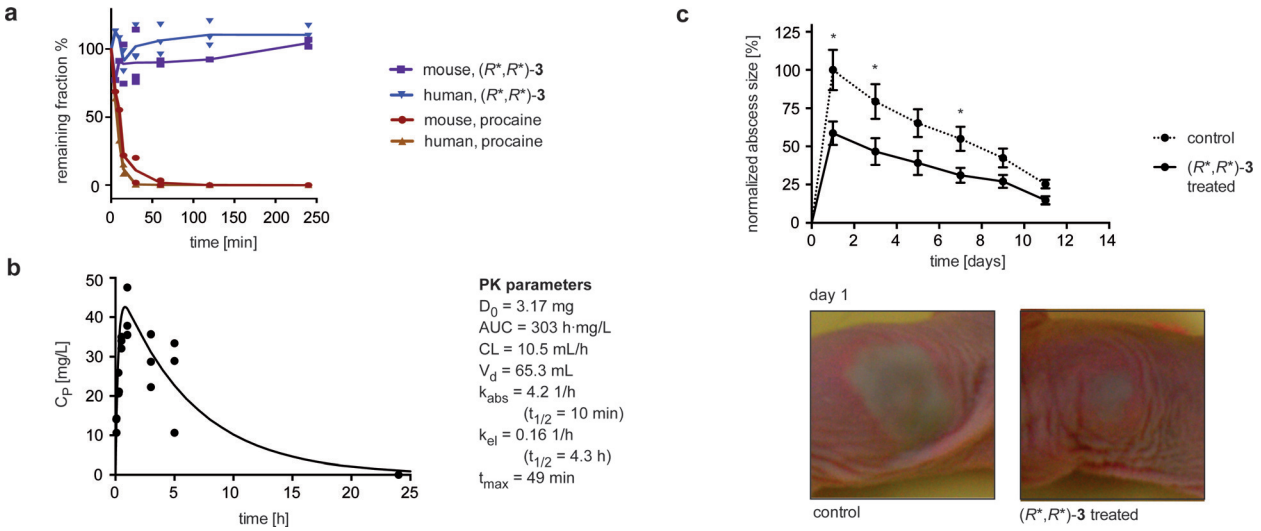

Figure 6. a) In vitro plasma levels of (*R**,*R**)-**3** remain stable for >4 h, whereas the positive control compound procaine is rapidly disintegrated. Three technical replicates are shown. b) In vivo pharmacokinetic parameters were determined following a single-dose i.p. injection of 3.17 mg (*R**,*R**)-**3** in corn oil. The group size comprised four mice ($n=4$) using three groups and an alternating blood withdrawal scheme. c) Systemic treatment of skin infections with compound (*R**,*R**)-**3** significantly ($^*p<0.05$) decreased the size of lesions induced by *S. aureus* USA 300 BAA-1717 (antihemolytic activity of (*R**,*R**)-**3** in this strain is shown in the Supporting Information, Figure S1 a). Graphs represent abscess sizes normalized to control animals at day one for control- and (*R**,*R**)-**3**-treated animals monitored over 13 days post-infection. All results are shown as mean values ± SEM for $n=32$ animals from four independent experiments. During the course of the experiments with *S. aureus* BAA-1717, six animals died prematurely (two control animals and four (*R**,*R**)-**3** treated animals).

Mode of action analysis: Transcriptome analysis was performed by RNA-seq analysis described by Dugar et al.[43] Target identification was performed with AfBPP[32] using photo-probes and quantitative dimethyl-labeling for mass-spectrometry, as previously described.[36] Validation experiments include functional studies of transposon mutants (Nebraska Transposon Mutant Library).

Conflict of interest: S. Sieber, T. Böttcher, K. Lorenz-Baath, O. Baron, V. Korotkov, F. Weinandy are named inventors on a patent ("Beta-O/S/N fatty acids and derivatives as anti-virulence drugs") related to this study. S. Sieber, O. Baron, T. Böttcher founded a company (AVIRU).

Keywords: click chemistry · drug discovery · proteomics · medicinal chemistry · toxicology

Acknowledgements

We thank the Network on Antimicrobial Resistance in *Staphylococcus aureus* (NARSA) for the supply of the Nebraska Transposon Mutant Library (NTML). Furthermore, we thank Professor Markus Gerhard for excellent scientific advice and the permission to perform animal experiments in his group at the Institute of Medical Microbiology, Immunology and Hygiene (Technische Universität München) as well as for the supply of clinical isolates. Animal studies were approved by the Government of Upper Bavaria under the accreditation number 55.2-1/54-2531-114/10. The work was funded by an ERC starting grant (250924-antibacterials) and by the Federal Ministry of Education and Research, Germany, FKZ: 031A131. The authors account for the content of the work. We would also like to thank Josef Schachtner for contribution to the synthesis of photoreactive chemical probes and Dr. Malte Gersch for an introduction to ABPP. Finally, we thank Ernst Bernges, Heike Hofmann, Mona Wolff, Burghard Cordes, and Katja Bäuml for excellent technical support.

[1] CDC Antibiotic resistance threats in the United States, U.S. Department of Health and Human Services, Centers for Disease Control and Prevention, **2013**.
[2] M. M. Mwangi, S. W. Wu, Y. Zhou, K. Sieradzki, H. de Lencastre, P. Richardson, D. Bruce, E. Rubin, E. Myers, E. D. Siggia, A. Tomasz, *Proc. Natl. Acad. Sci. USA* **2007**, *104*, 9451 – 9456.
[3] A. E. Clatworthy, E. Pierson, D. T. Hung, *Nat. Chem. Biol.* **2007**, *3*, 541 – 548.
[4] D. A. Rasko, V. Sperandio, *Nat. Rev. Drug Discovery* **2010**, *9*, 117 – 128.
[5] S. Ruer, N. Pinotsis, D. Steadman, G. Waksman, H. Remaut, *Chem. Biol. Drug Des.* **2015**, *86*, 379 – 399.
[6] D. T. Hung, E. A. Shakhnovich, E. Pierson, J. J. Mekalanos, *Science* **2005**, *310*, 670 – 674.
[7] D. A. Rasko, C. G. Moreira, D. R. Li, N. C. Reading, J. M. Ritchie, M. K. Waldor, N. Williams, R. Taussig, S. Wei, M. Roth, D. T. Hughes, J. F. Huntley, M. W. Fina, J. R. Falck, V. Sperandio, *Science* **2008**, *321*, 1078 – 1080.
[8] V. Khodaverdian, M. Pesho, B. Truitt, L. Bollinger, P. Patel, S. Nithianantham, G. Yu, E. Delaney, E. Jankowsky, M. Shoham, *Antimicrob. Agents Chemother.* **2013**, *57*, 3645 – 3652.
[9] F. Tang, W.-H. Li, X. Zhou, Y.-H. Liu, Z. Li, Y.-S. Tang, X. Kou, S.-D. Wang, M. Bao, L.-D. Qu, M. Li, B. Li, *Microb. Drug Resist.* **2014**, *20*, 357 – 363.
[10] R. C. Allen, R. Popat, S. P. Diggle, S. P. Brown, *Nat. Rev. Microbiol.* **2014**, *12*, 300 – 308.
[11] G. Y. Liu, A. Essex, J. T. Buchanan, V. Datta, H. M. Hoffman, J. F. Bastian, J. Fierer, V. Nizet, *J. Exp. Med.* **2005**, *202*, 209 – 215.
[12] C. I. Liu, G. Y. Liu, Y. Song, F. Yin, M. E. Hensler, W. Y. Jeng, V. Nizet, A. H. Wang, E. Oldfield, *Science* **2008**, *319*, 1391 – 1394.
[13] Y. Song, C. I. Liu, F. Y. Lin, J. H. No, M. Hensler, Y. L. Liu, W. Y. Jeng, J. Low, G. Y. Liu, V. Nizet, A. H. Wang, E. Oldfield, *J. Med. Chem.* **2009**, *52*, 3869 – 3880.
[14] J. Qiu, X. Niu, J. Dong, D. Wang, J. Wang, H. Li, M. Luo, S. Li, H. Feng, X. Deng, *J. Infect. Dis.* **2012**, *206*, 292 – 301.
[15] F. Weinandy, K. Lorenz-Baath, V. S. Korotkov, T. Bottcher, S. Sethi, T. Chakraborty, S. A. Sieber, *ChemMedChem* **2014**, *9*, 710 – 713.

[16] J. Zhang, H. Liu, K. Zhu, S. Gong, S. Dramsi, Y. T. Wang, J. Li, F. Chen, R. Zhang, L. Zhou, L. Lan, H. Jiang, O. Schneewind, C. Luo, C. G. Yang, *Proc. Natl. Acad. Sci. USA* **2014**, *111*, 13517 – 13522.
[17] M. Otto, *Expert Opin. Biol. Ther.* **2010**, *10*, 1049 – 1059.
[18] G. Y. C. Cheung, M. Otto, *Expert Opin. Ther. Targets* **2012**, *16*, 601 – 612.
[19] E. A. George, T. W. Muir, *ChemBioChem* **2007**, *8*, 847 – 855.
[20] R. P. Novick, *Mol. Microbiol.* **2003**, *48*, 1429 – 1449.
[21] E. A. George, R. P. Novick, T. W. Muir, *J. Am. Chem. Soc.* **2008**, *130*, 4914 – 4924.
[22] Y. Tal-Gan, D. M. Stacy, M. K. Foegen, D. W. Koenig, H. E. Blackwell, *J. Am. Chem. Soc.* **2013**, *135*, 7869 – 7882.
[23] E. J. Murray, R. C. Crowley, A. Truman, S. R. Clarke, J. A. Cottam, G. P. Jadhav, V. R. Steele, P. O'Shea, C. Lindholm, A. Cockayne, S. R. Chhabra, W. C. Chan, P. Williams, *J. Med. Chem.* **2014**, *57*, 2813 – 2819.
[24] Y. Chien, A. C. Manna, S. J. Projan, A. L. Cheung, *J. Biol. Chem.* **1999**, *274*, 37169 – 37176.
[25] A. C. Manna, A. L. Cheung, *J. Bacteriol.* **2006**, *188*, 4288 – 4299.
[26] T. Böttcher, S. A. Sieber, *J. Am. Chem. Soc.* **2008**, *130*, 14400 – 14401.
[27] E. Zeiler, V. S. Korotkov, K. Lorenz-Baath, T. Bottcher, S. A. Sieber, *Bioorg. Med. Chem.* **2012**, *20*, 583 – 591.
[28] S. W. Cho, D. Romo, *Org. Lett.* **2007**, *9*, 1537 – 1540.
[29] D. W. Huang, B. T. Sherman, R. A. Lempicki, *Nat. Protoc.* **2008**, *4*, 44 – 57.
[30] D. W. Huang, B. T. Sherman, R. A. Lempicki, *Nucleic Acids Res.* **2009**, *37*, 1 – 13.
[31] A. L. Cheung, A. S. Bayer, G. Zhang, H. Gresham, Y. Q. Xiong, *FEMS Immunol. Med. Microbiol.* **2004**, *40*, 1 – 9.
[32] M. J. Evans, B. F. Cravatt, *Chem. Rev.* **2006**, *106*, 3279 – 3301.
[33] R. Huisgen, *Proc. Chem. Soc.* **1961**, 357 – 396.
[34] V. V. Rostovtsev, L. G. Green, V. V. Fokin, K. B. Sharpless, *Angew. Chem. Int. Ed.* **2002**, *41*, 2596 – 2599; *Angew. Chem.* **2002**, *114*, 2708 – 2711.
[35] C. W. Tornøe, C. Christensen, M. Meldal, *J. Org. Chem.* **2002**, *67*, 3057 – 3064.
[36] J. L. Hsu, S. Y. Huang, N. H. Chow, S. H. Chen, *Anal. Chem.* **2003**, *75*, 6843 – 6852.
[37] *Uni*Prot, *Nucleic Acids Res.* **2015**, 43, D204 – D212.
[38] H. J. Tseng, Y. Srikhanta, A. G. McEwan, M. P. Jennings, *Mol. Microbiol.* **2001**, *40*, 1175 – 1186.
[39] K. M. Papp-Wallace, M. E. Maguire, *Annu. Rev. Microbiol.* **2006**, *60*, 187 – 209.
[40] B. A. Diep, Q. Phung, S. Date, D. Arnott, C. Bakalarski, M. Xu, G. Nakamura, D. L. Swem, M. K. Alexander, H. N. Le, T. T. Mai, M.-W. Tan, E. J. Brown, M. Nishiyama, *J. Infect. Dis.* **2014**, *209*, 1533 – 1541.
[41] M. J. Horsburgh, S. J. Wharton, A. G. Cox, E. Ingham, S. Peacock, S. J. Foster, *Mol. Microbiol.* **2002**, *44*, 1269 – 1286.
[42] T. E. Kehl-Fie, Y. Zhang, J. L. Moore, A. J. Farrand, M. I. Hood, S. Rathi, W. J. Chazin, R. M. Caprioli, E. P. Skaar, *Infect. Immun.* **2013**, *81*, 3395 – 3405.
[43] G. Dugar, A. Herbig, K. U. Forstner, N. Heidrich, R. Reinhardt, K. Nieselt, C. M. Sharma, *PLoS Genet.* **2013**, *9*, e1003495.

Received: October 5, 2015
Published online on January 8, 2016